Relative Role of Dynamic and Thermodynamic Processes in the Development of the Indian Ocean Dipole: An OGCM Diagnosis

Tim Li, Yongsheng Zhang, Er Lu, and Dailin Wang

International Pacific Research Center, School of Ocean and Earth Science and Technology, University of Hawaii, Honolulu, Hawaii

Abstract. The relative role of oceanic dynamics and surface heat fluxes in the initiation and development of the Indian Ocean dipole was investigated by analyzing results from an oceanic general circulation model. The model was forced by observed surface wind stress and heat flux fields for 1958-1997. The results show that it was capable of reproducing observed dipole events over the tropical Indian Ocean. The diagnosis of the mixed-layer heat budget indicates that the SST anomaly (SSTA) in the east pole is primarily induced by anomalous surface latent heat flux and vertical temperature advection, whereas in the west pole it is mainly caused by meridional and vertical temperature advection anomalies. In both regions shortwave radiation anomalies tend to damp the SSTA. The ocean Rossby waves are essential in linking the anomalous wind and SST off Sumatra and subsurface temperature variations in southwest Indian Ocean.

1. Introduction

Extreme climate events occurred in 1997 across the Indo-Pacific Ocean. In the tropical Pacific the largest El Nino in the last 100 years took place. In the equatorial Indian Ocean (IO) a strong zonal SST dipole developed, with a cold SST anomaly (SSTA) and suppressed convection off Sumatra and a warm SSTA and enhanced convection in the western IO (Webster et al. 1999, Saji et al. 1999). Historically, there are a number of similar but weaker dipole events in the tropical IO, many of which coexisted with El Ninos (Reverdin et al. 1986, Hastenrath et al. 1993, Reason et al. 2000). In fact, the temporal correlation between the El Nino and IO dipole (IOD) in the past 40 years has prompted several investigators (e.g., Chambers et al. 1999, Murtugudde et al. 2000, Ueda and

Matsumoto 2000) to hypothesize that the IOD results from direct ENSO forcing. However, the IOD has a life cycle that is different from ENSO. For instance, El Nino often peaks in December-January, while the mature phase of the IOD occurs in October (Saji et al. 1999). Li et al. (2002) attributed this distinctive phase-locking feature to a seasonal-dependent positive thermodynamic air-sea feedback off Sumatra. The occurrence of some IOD events in non-El Nino years (such as in 1961 and 1994) implies that factors other than the remote El Nino forcing must come to play.

A key unanswered question is what is the relative role of ocean dynamics versus surface heat fluxes in the initiation and growth of the IOD. In the El Nino scenario, ocean thermocline displacement and associated subsurface temperature changes are essential in changing the SST, and the effect of surface heat fluxes is of second importance (Zebiak and Cane 1987). In the warm oceans such as the tropical IO, the mean thermocline is quite deep so that surface heat fluxes must play a role in changing the SST. The objective of this study is to understand the relative role of oceanic dynamic versus thermodynamic processes in the development of the IOD by means of an ocean general circulation model (OGCM).

2. The model and numerical experiments

The model data used in this analysis are from the second repeat of a 40-year (1958-1997) global ocean simulation conducted at the National Center for Atmospheric Research (NCAR), using the NCAR ocean model. The model resolution is 2.4 degrees in the zonal direction and variable in the meridional direction, from 0.6 degrees at the equator to 1.2 degrees at high latitudes. There are 45 levels in the vertical, with a grid-spacing of 8 m at the surface to 258 m at the bottom. The model employs the isopycnal mixing scheme of Gent and McWilliams (1990) and KPP vertical mixing of Large et al. (1994). Anisotropic horizontal viscosity is also employed to improve the simulation of the equatorial current system (Large et al. 2001). The heat flux forcing is that of the bulk

formulation of Large et al. (1997). The solar flux fields are derived from the ISCCP data for 1984-91 and the NCEP/NCAR reanalysis for other periods. The four times daily wind stress is derived from the NCEP/NCAR reanalysis data. A blended precipitation is derived from MSU and Xie-Arkin (1996) observations for 1979-1993. For other periods the climatological precipitation is used. The reason to use the blended precipitation data is to reduce the excessive tropical precipitation of Xie-Arkin (1996) while retaining its low precipitation at high latitudes.

3. Composite IOD structures and the mixed-layer heat budget

Figure 1a shows the time series of both observed and simulated dipole mode indices defined as SSTA differences between the western and eastern IO, following Saji et al. (1999). The model is capable of reproducing the observed dipole events in the past 40 years. The correlation between the two time series is 0.7. To further examine the model performance in simulating the horizontal structure of the IOD, we conducted a composite analysis based on 6 major IOD events in the past 40 years (i.e., the 1961, 1967, 1972, 1982, 1994 and 1997 events). The seasonal progression of the composite SSTA patterns is illustrated in Fig. 1b. The gross pattern and evolution of the model IOD are similar to the observed. The IOD is initiated in late spring, develops rapidly in summer, and reaches its mature phase in northern fall.

Given that the OGCM is capable of simulating the spatial and temporal structures of the IOD, we investigate processes that are responsible for the initiation and growth of the dipole. Figure 2 shows the composites of the surface wind, net shortwave radiation, and latent heat flux. The surface wind anomaly in MAM is characterized by a weak southeasterly along the coast of Sumatra. The anomalous wind is intensified in boreal summer. It is likely that the enhanced southeasterly results from a strengthened monsoon over the western North Pacific (WNP). It is noted that an anomalous cyclone appears over the WNP in boreal summer. The enhanced monsoon convection

may induce northward cross-equatorial winds and enhance the southeasterly along the coast of Sumatra. Thus, the WNP monsoon may play a role in strengthening the cold SSTA in the east pole. Similar anomalous wind patterns appear during the austral winter and spring of El Nino composites (Reason et al. 2000), suggesting a remote forcing mechanism from the eastern Pacific. Another possible process that enhances the southeasterly is through the enhanced convection in the central and western equatorial IO (Saji et al. 1999, Webster et al. 1999). By SON, the anomalous southeasterly reaches maximum amplitude, and a closed anticyclone cell appears in the southern IO.

The surface latent heat flux anomaly contributes greatly to the SST cooling in the east pole during the initial development. It has a cooling maximum about 1000 km offshore in MAM and JJA (Fig. 2b). The shortwave radiation anomaly has a maximum amplitude in SON over the seas adjacent to Java-Sumatra (Fig. 2c). It tends to suppress the SSTA in situ, owing to a negative cloud-radiation-SST feedback (Ramanathan and Collins 1991).

In general, the change of SST is caused by both surface heat fluxes and 3-dimensional ocean temperature advection. To assess the relative role of the dynamic and thermodynamic processes, we diagnose the ocean mixed-layer heat budget in which we take into account the effect of the mixed-layer depth change. The time change rate of the mixed-layer-averaged temperature may be written as

$$\frac{?<T>}{?t} = -<u\frac{?T}{?x}> -<v\frac{?T}{?y}> -<w\frac{?T}{?z}> + \frac{Q_{SW} - Q_{LW} - Q_{LH} - Q_{SH}}{\rho c_w h} + R \qquad (1)$$

where u, v and w are three-dimensional ocean current velocities, Q_{SW}, Q_{LW}, Q_{LH} and Q_{SH} represent the net downward shortwave radiation at the ocean surface, net upward longwave radiation, surface latent and sensible heat fluxes, R is a residual term representing either the model errors or processes other than heat fluxes and temperature advection, ρ is the density of water, c_w denotes the specific heat of water, and h represents the depth of the mixed layer that changes in

space and time. (h is defined as a depth at which ocean temperature is a half degree lower than that at the surface.) For a variable A, <A> is defined as the vertical average of A from the ocean surface to the bottom of the mixed layer, that is, $<A>=\frac{1}{h}\int_0^h A dz$. Once each term in (1) is calculated, anomaly fields are derived by subtracting total fields from climatological annual cycle fields. Finally a horizontal average is performed for the east and west pole regions as defined by Saji et al. (1999).

Figure 3 shows the mixed-layer heat budgets for both the east and west poles. The sum of 3-d temperature advection and heat flux terms well represents the time tendency of the mixed-layer temperature anomalies in both regions (Fig. 3a), and the residual terms are quite small. At the east pole, the initial cooling is mainly attributed to anomalous surface latent heat flux associated with enhanced southeasterly flow along the coast of Sumatra (Fig. 3c). At the time of maximum cooling tendency (i.e., at lags –1 and –2), the shortwave and latent fluxes nearly balance out, while the effect of the ocean temperature advection increases. The SSTA develops rapidly in boreal summer, owing to a positive thermodynamic feedback[1] and the enhancement of the WNP monsoon. Both processes enhance the southeasterly along the coast of Sumatra. The enhanced southeasterly further increases the cold SSTA in situ through enhanced surface evaporation, vertical mixing, and coastal upwelling.

While the latent heat flux anomaly leads the SSTA for a few months, the anomalous vertical temperature advection tends to be in phase with the SSTA (Fig. 3b), owing to a positive feedback between anomalous wind and ocean upwelling/thermocline depth displacement. In response to the east-west SSTA gradient, maximum easterly anomalies appear in the central equatorial IO. The

[1] In their submitted papers, Li et al. (2002) and Wang et al. (2002) proposed a positive feedback mechanism between an anomalous atmospheric anticyclone and a cold SSTA off Sumatra.

easterly anomalies induce anomalous ocean upwelling and shallower thermocline in the eastern equatorial IO, leading to the increase of the cold SSTA there. This leads to an increase of the zonal SSTA gradient. As a result of this positive air-sea feedback, the anomalous vertical temperature advection is in phase with the SSTA.

The anomalous horizontal temperature advection also contributes to the development of the SSTA in the east pole. The zonal advection anomaly, which is slightly greater than the meridional advection anomaly, leads the SSTA by one month. It also contributes somewhat to the decaying of the SSTA after the IOD matures, although its magnitude is weaker than the solar and latent heat flux anomalies.

Different from the east pole, the SSTA in the west pole is primarily induced by ocean dynamics. Figure 3b shows that both anomalous vertical and meridional temperature advections contribute greatly to the anomalous warming in the western IO. The effect of the latent heat flux anomaly is modest due to weak surface wind speeds in the region (see Fig. 2a). The effect of ocean dynamics in the west pole was previously suggested by Webster et al. (1999).

The change of depth of the mixed layer greatly modulates the heat flux effect on the SSTA. Figure 3d illustrates the time evolution of the composite mixed-layer depth in both the east and west poles. The mixed layer depth changes rapidly during the development of the IOD in both regions. It drops about 15 m from lag –2 to lag 0. This means that the effect of the surface heat fluxes increases 30% during that period.

A unique feature in the tropical IO is the appearance of a minimum center of the mean thermocline depth (represented by 20?C isotherm depth) south of the equator (near 60?E and 10?S, Fig. 4a). The formation of this minimum center is attributed to the curl of the annual mean wind stress between the equatorial westerly and the easterly in the subtropical southern IO (Xie et al.

2002). The greatest interannual variability is located south of this minimum center in the middle of the strong meridional depth gradient associated with the South Equatorial Current (Fig. 4b). Another strong interannual variability center is located in the southeastern IO off Sumatra. Variations of thermocline depth and subsurface temperature anomalies in both regions are dynamically linked. The maximum lagged correlation between subsurface temperatures at 50 m in the two regions is –0.7. The physical linkage between the two variability centers is through the propagation of ocean Rossby waves, as illustrated in Fig. 4c. The curl of the anomalous wind stress off Sumatra forces a host of ocean Rossby waves, which carry the signal of deeper thermocline depth anomalies and propagate westward. The subsurface temperature signals associated with the thermocline depth anomalies are amplified in the southwest IO where the mean thermocline is shallow. The westward propagation of ocean Rossby waves was clearly detected in 1997-98 by satellite measurements (Webster et al. 1999). It is likely that these Rossby waves are not pure free waves (due to their slow phase propagation speed), and they may arise from a coupling between the tropical atmosphere and ocean (Xie et al. 2002).

4. Concluding remarks

The relative role of dynamic and thermodynamic processes in the initiation and development of the Indian Ocean dipole was investigated by the diagnosis of output of an OGCM. Forced by observed surface wind stress and heat fluxes, the OGCM is capable of reproducing the observed IOD events in the past 40 years. A strategy is developed to analyze the mixed-layer heat budget by taking into account the effect of variability of the ocean mixed layer depth.

Our results indicate that dominant processes that contribute to the development of the SSTA in the east pole are the anomalous latent heat fluxes and vertical temperature advection. The former leads the surface cooling by a few months, and the latter is in phase with the SSTA. The SSTA in the

west pole is primarily induced by 3-dimensional temperature advection that includes the remote effect of ocean Rossby waves generated by the curl of anomalous wind stress off Sumatra. The greatest thermocline and subsurface temperature variability appears in the southwest IO (near 10?S) where the annual mean thermocline is shallow. Another variability center is found in the southeast IO off Sumatra. In both east and west poles, the shortwave radiation anomaly acts as a negative feedback agent to damp the original SSTA. The anomalous WNP monsoon may contribute to the rapid development of the IOD in boreal summer through induced cross-equatorial winds that enhance the southeasterly off Sumatra.

The results presented above are from a stand-alone ocean model. Further studies are needed to understand atmosphere-ocean feedback processes in a coupled model.

Acknowledgments. The authors acknowledge NCAR for providing the ocean model data. Discussions with Drs. Bin Wang and C.-P. Chang are greatly appreciated. This work was supported by the NSF Grant ATM01-19490 and NOAA Grant NA01AANRG0011. The International Pacific Research Center is in part sponsored by the Frontier Research System for Global Change. This is SOEST contribution number 6029 and IPRC contribution number 175.

References

Chambers, D.P., B.D. Tapley, and R.H. Stewart, Anomalous warming in the Indian Ocean coincident with El Nino. *J.Geophys.Res*., **104**, 10523-10533, 1999.

Gent, P.R. and J.C. McWilliams, Isopycnal mixing in ocean circulation models. *J. Phys. Oceanogr.*, **20**, 150-155, 1990.

Hastenrath, S., A. Nicklis, and L. Greischar, Atmospheric-hydrospheric mechanisms of climate anomalies in the western equatorial Indian Ocean. *J. Geophys. Res*., **98**, 20219-20235, 1993.

Large, W. G., J.C. McWilliams, and S.C. Doney, Oceanic vertical mixing: A review and a model with a nonlocal boundary layer parameterization. *Rev. Geophys*., **32**, 363-403, 1994.

_____, G. Danabasoglu, S.C. Doney, and J.C. McWilliams, Sensitivity to surface forcing and boundary layer mixing in a global ocean model: Annual mean climatology. *J. Phys. Oceanogr*., **27**, 2418-2447, 1997.

_____, _____, J.C. McWilliams, P.R. Gent, and F.O. Bryan, Equatorial Circulation of a Global Ocean Climate Model with Anisotropic Horizontal Viscosity. *J. Phys. Oceanogr*., **31**, 518-536, 2001.

Li, T., B. Wang, C.-P. Chang, and Y.S. Zhang, A theory for the Indian Ocean dipole mode. *J.Atmos.Sci*., submitted, 2002.

Murtugudde, R., J.P. McCreary Jr, A.J. Busalacchi, Oceanic processes associated with anomalous events in the Indian Ocean with relevance to 1997-1998. *J. Geophy. Res*., **105**, 3295-3306, 2000.

Reason, C. J. C, Allan R. J, Lindsay J. A and Ansell T. J, ENSO and climatic signals across the Indian Ocean Basin in the global context: Part I, interannual composite patterns, International Journal of Climatology, 20(11), 1285-1327, 2000.

Ramanathan, V., and W. Collins, Thermodynamic regulation of ocean warming by cirrus clouds deduced from observations of the 1987 El Nino. *Nature*, **351**, 27-32, 1991.

Reverdin, G., D.L. Cadet, and D. Gutzler, Interannual displacement of convection and surface circulation over the equatorial Indian Ocean. *Quart.J.Roy.Met.Soc*., **112**, 43-67, 1986.

Saji, N.H., B.N. Goswami, P.N. Vinayachandran, and T. Yamagata, A dipole mode in the tropical Indian Ocean. *Nature*, **401**, 360-363, 1999.

Ueda, H., and J. Matsumoto, A possible process of east-west asymmetric anomalies over the Indian Ocean in relation to 1997/98 El Nino. *J.Meteor.Soc.Japan*, Vol. **78**78

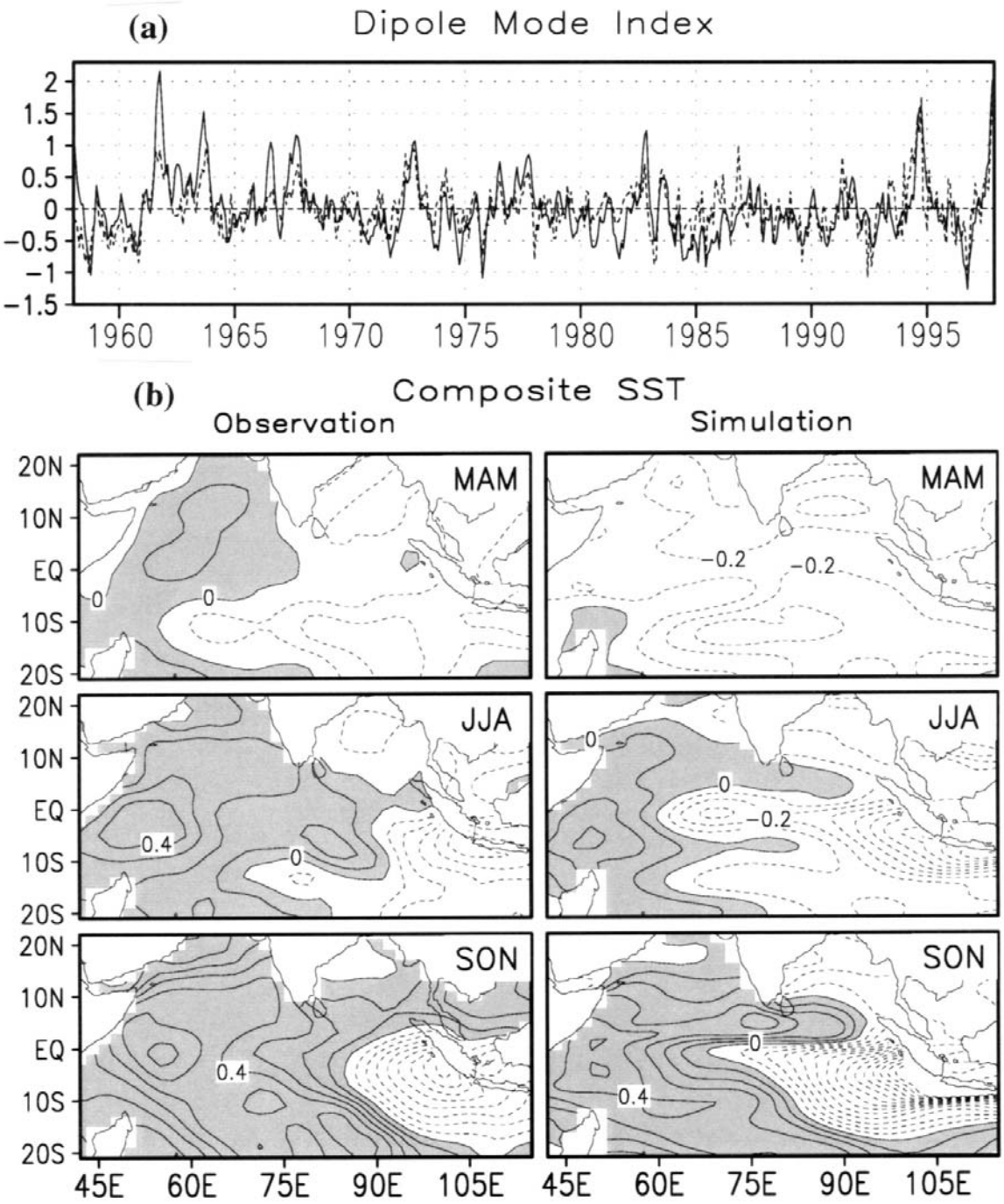

Fig. 1 (a) Time evolution of the observed (dashed line) and simulated (solid line) dipole mode index. The dipole model index is defined as the SSTA difference (?C) between the western and eastern equatorial Indian Ocean as defined by Saji et al. (1999). (b) Structure and evolution of observed and simulated composite SSTA (?C) in MAM, JJA and SON. The composite is based on the six major dipole events in 1961, 67, 72, 82, 94, and 97. Shaded regions denote the positive SSTA.

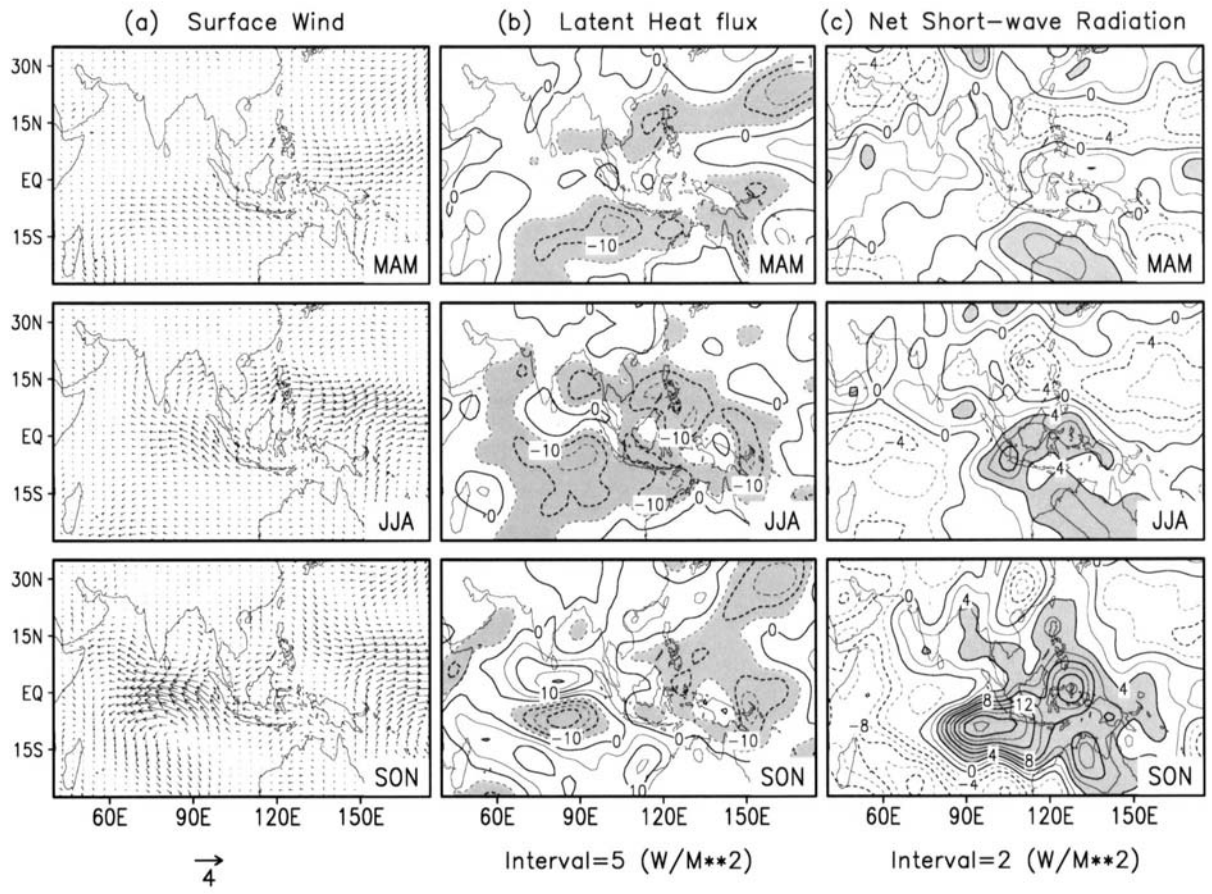

Fig. 2 Evolution of composites of (a) the surface wind (units: ms^{-1}), (b) surface latent heat flux (units: Wm^{-2}) and (c) net surface shortwave radiation (units: Wm^{-2}) in MAM, JJA, and SON. The composite is based on the six major dipole events in 1961, 67, 72, 82, 94, and 97.

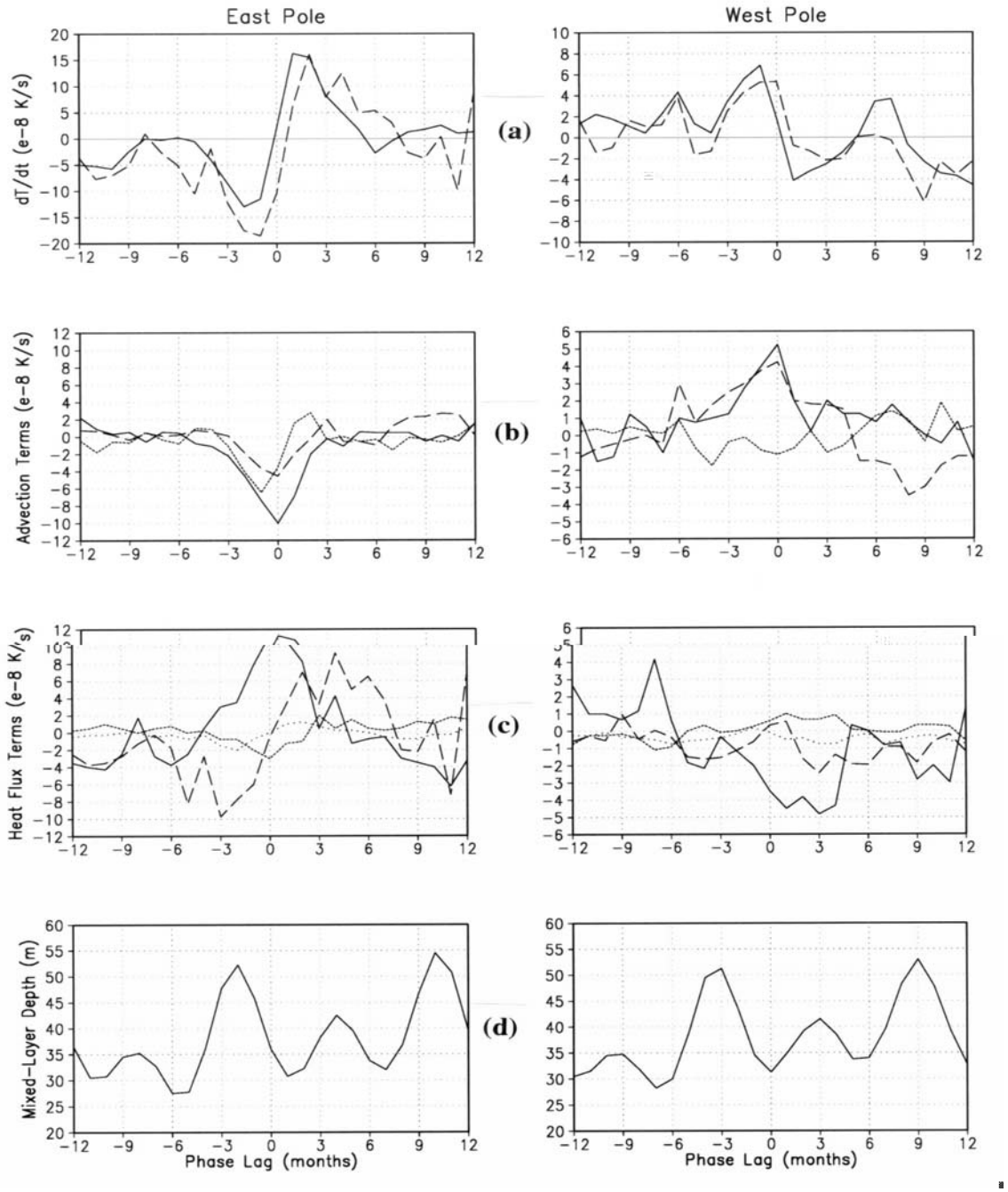

Fig. 3 (a) Composite mixed layer temperature tendencies (units: $10^{-8} Ks^{-1}$, solid line) and contributions from the sum of ocean advection and heat flux terms (dashed line), (b) tendencies due to anomalous zonal (short-dashed line), meridional (long- dashed line) and vertical (solid line) temperature advection, (c) tendencies due to shortwave radiation (solid line), latent heat flux (long-dashed line), longwave radiation (short-dashed line) and sensible heat flux (dot line), and (d) evolution of the oceanic mixed layer depth (m) for the east pole (left panels) and west pole (right panels). The composite is based on the same six dipole events as in Fig. 1. Phase lag 0 corresponds to the mature phase of the IOD in October.

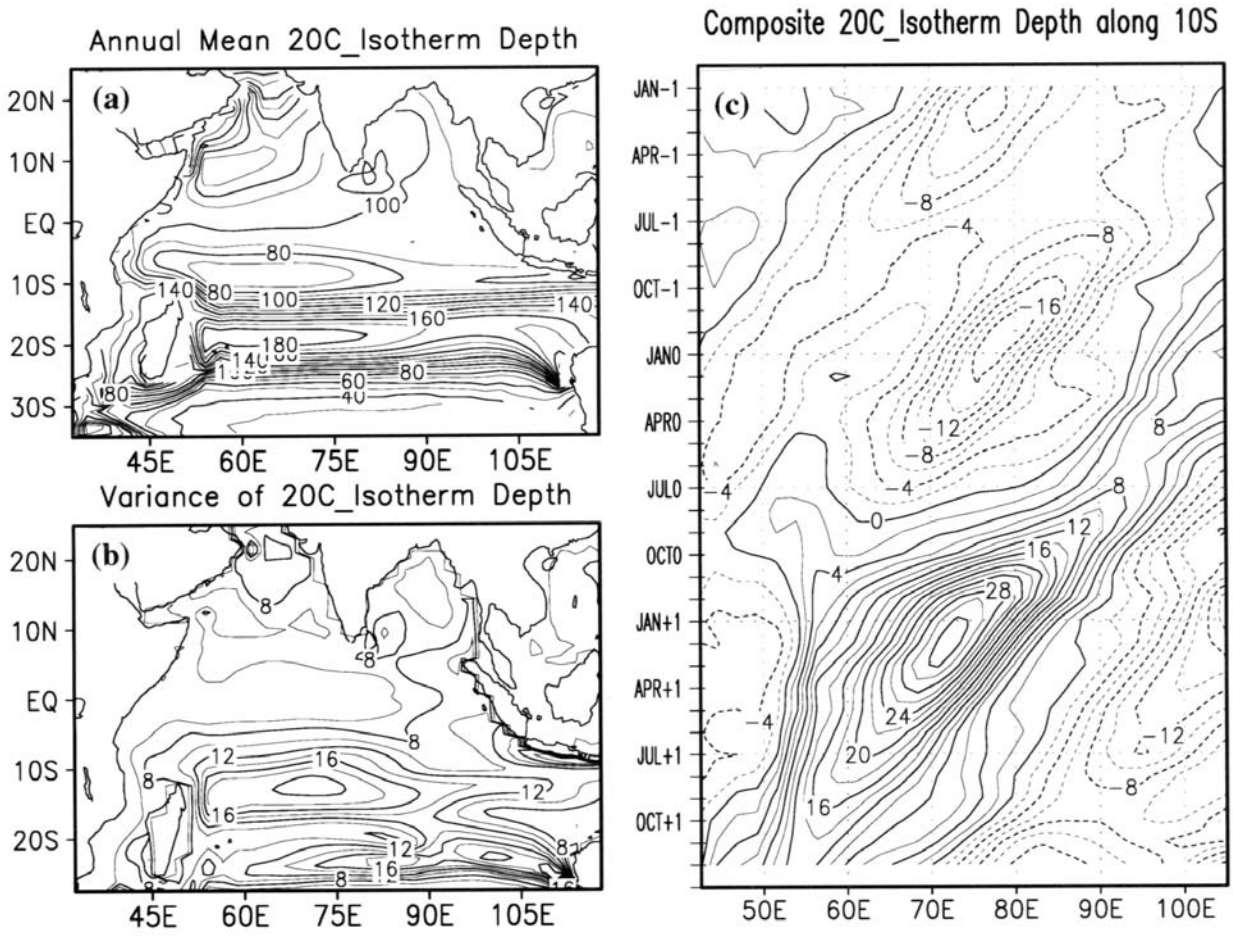

Fig. 4 (a) Horizontal distribution of the model annual mean 20?C isotherm depth (top left panel, units: m), (b) variance of the model 20?C isotherm depth anomaly (lower left panel), and (c) longitude-time section of the model composite 20?C isotherm depth anomaly (m) at 10?S. The composite is based on the same six dipole events as in Fig.1. “-1”, “0”, and “+1” represent the year before, during, and after a dipole event.